Chapter 2
Classical Density Functional Theory of Ionic Solutions

Jan Forsman, Clifford E. Woodward and Ryan Szparaga

Abstract The basic structure of classical density functional theory (DFT) is reviewed from a rather general perspective. The treatment is then specialized to ionic solutions, describing the various possible extensions beyond the Poisson–Boltzmann level, that DFT offers, such as excluded volume effects, non-electrostatic interactions, connectivity (polymers) and ion correlations. The last effects are discussed rather thoroughly, with several explicit illustrations.

2.1 Introduction

Interactions between charged surfaces are important in almost all areas of colloid and surface science, including biological systems. A convenient, albeit approximate, way to model these systems is to treat the solvent implicitly as a dielectric continuum with a fixed dielectric constant and the charged species as spheres with appropriate valency. This simplified model is then often approximately solved using the Poisson–Boltzmann approximation (PBA). The PBA derives from a mean-field treatment of the Coulombic forces, and is often expressed as a non-linear differential equation. Its linearized form, the Debye–Hückel theory, is valid in cases where the coupling is small. Over the years, a lot of effort has been devoted to solving the PBA in the presence of various geometrical constraints. A much more versatile formulation of the PBA is arrived at from the point of view of *classical* density functional theory, DFT. Here, the system free energy is expressed as a functional of the ion distributions. By using a mean-field approximation to the Coulombic energy, and ignoring short-ranged effects, one quite naturally arrives at the PBA. Advantages of a DFT formulation of these systems include:

J. Forsman (✉) · R. Szparaga
Theoretical Chemistry, Chemical Centre, P.O. Box 124, 221 00 Lund, Sweden
e-mail: jan.forsman@teokem.lu.se

C.E. Woodward
School of Physical, Environmental and Physical Sciences, University College, University of New South Wales, ADFA, Canberra, ACT 2600, Australia

© Springer International Publishing Switzerland 2015

W. Rocchia and M. Spagnuolo (eds.), *Computational Electrostatics for Biological Applications*, DOI 10.1007/978-3-319-12211-3_2

- An explicit expression for the free energy allows for a more straightforward implementation of thermodynamic consistency checks, e.g. the contact value theorem (see below), which is also useful for debugging computer code.
- Evaluation of the free energy is extremely useful for studies involving phase equilibria and/or surface interactions.
- The DFT has explicit separate expressions for the entropy and energy. The latter includes the specific intermolecular interactions, which allows straightforward extension of the PBA to model systems with forces in addition to electrostatic ones, e.g. hard core and dispersion interactions.
- In the DFT formalism, the PBA is easily generalized to treat more complex models, such as charged polymers of various architectures [1, 2], polydispersity [3] and even titrating molecules [4].
- Extending the theory beyond the PBA to include ion correlations (which in some systems are of vital importance) can often be carried out within the DFT, using phenomenological approaches that are remarkably accurate [1, 5–8].
- Finally, hybrid schemes combining DFT and computer simulations can also be used to account for intramolecular correlations, otherwise missing in the basic DFT free energy.

On the other hand, the DFT approach also carries some disadvantages:

- It is not widely used, and there are few available software packages.
- The efficiency of DFT is not as well tested for cases where the system has no simple symmetry to allow one to reduce the dimensionality of the problem, although there are examples of such studies [9–11].

We expect that many readers of this book are primarily familiar with the differential equation approach to the PBA. Hence, we will firstly describe classical DFT in a rather general framework, with a subsequent focus on ionic solutions.

2.2 Classical DFT of Simple Fluids

In order to simplify the notation at this stage, we will limit our treatment to simple spherical particles. Extensions to polymers, stars, etc., are relatively straightforwardly [12] carried out within the DFT formalism. As is well known the *configurational integral*, Z, of an interacting classical system, contains all the equilibrium thermodynamic information. Denoting the inverse thermal energy by β, this integral is (for an N-particle system) defined as:

$$Z = \int e^{-\beta U(\mathbf{r}^N)} \, \mathrm{d}\mathbf{r}^N \tag{2.1}$$

Here, U is the interaction energy, while $\mathbf{r}^N \equiv \mathbf{r}_1, ..., \mathbf{r}_N$, represents a particular configuration, with $\mathbf{r}_i$ the coordinate of particle i. Evaluating the configurational integral

is not easily carried out via computer simulation methods, which lend themselves to the calculation of thermodynamic averages instead. Even then, an assumption of *pairwise additivity* for the interactions is most often invoked.

Computer simulations allow us to *in principle* obtain exact thermodynamic averages (subject to statistical noise), in the thermodynamic limit, provided our simulation system contains a sufficient number of particles, so boundary effects are negligible. Simulating a large enough system may be an exceptionally demanding task, or even impossible in practice. Additionally, the model itself is often a very crude representation of the reality. Given these difficulties, it might be worthwhile to consider a more approximate, but computationally faster approach, which would still provide qualitative, or even semi-quantitative results. Such an approach would also provide inroads into studies of even more complex systems, such as solutions wherein the solvent is treated explicitly, or contain long polymer chains. The DFT attempts to evaluate the system free energy (essentially the natural logarithm of Z) directly, using simplifying approximations. Other thermodynamic properties, such as the entropy and average energy can then be easily obtained from this free energy.

2.2.1 The Generalized van der Waals' Theory

An example of a DFT approach is the "*generalized van der Waals' theory*" pioneered by Nordholm and co-workers [13–17]. This theory was able to capture packing effects in heterogeneous environments by the use of a non-local averaging (or measure) of the particle density. As the name suggests, it is based on the original ideas of van der Waals [18], supplemented with more accurate estimates of the hard core entropy.

Consider a single-component N-particle system which interact via spherically symmetric pair potentials, denoted $\phi(r)$. This means that the interaction between a "tagged" particle and another one a distance r away, is given by $\phi(r)$. Initially, we shall assume that the density, $n(r)$, around the tagged particle is uniform and equal to the overall bulk density, i.e. $n(r) = n_b$. That is, we neglect correlations between the particles, which is the nature of a *mean-field* approximation. The mean-field assumption dramatically simplifies the calculation of the configurational integral, Z. The(mean-field) energy per particle, e_p^{MF}, can be written as:

$$e_p^{\mathrm{MF}} = \frac{1}{2} n_b \int_0^\infty 4\pi r^2 \phi(r)\, \mathrm{d}r \tag{2.2}$$

From a technical point of view, we note that such an integral may diverge for the case where particles have an infinitely repulsive core. This will not be the case for the purely Coulomb interaction, but for other types of interactions, such as hard spheres or Lennard–Jones interactions a proper treatment of the core contribution is necessary (as discussed later). The total interaction energy, U^{MF}, is simply N times the energy per particle: $U^{\mathrm{MF}} = N 2\pi n_b \int_0^\infty r^2 \phi(r)$. Hence, we can write:

$$Z^{\mathrm{MF}} = \int e^{-\beta U}\,\mathrm{d}\mathbf{r}^N = e^{-\beta U^{\mathrm{MF}}} \int \mathbf{r}^N = V^N e^{-\beta N 2\pi n_b \int_0^\infty r^2 \phi(r)\,\mathrm{d}r} \tag{2.3}$$

where V is the volume. Note that we do not consider the kinetic part of the partition sum, which can be obtained analytically. The configurational Helmholtz free energy is given by $\beta\mathscr{F} = -\ln[Z/N!]$ and the mean-field approximation is, $\mathscr{F}^{\mathrm{MF}}$, which can also be written as:

$$\frac{\beta\mathscr{F}^{\mathrm{MF}}}{V} = n_b \ln[n_b] - n_b + 2\pi\beta n_b^2 \int_0^\infty r^2 \phi(r)\,\mathrm{d}r \tag{2.4}$$

where we have used Stirling's Approximation for $N!$. Strictly speaking, the communal entropy term, given by the second term in the equation above, is absent in the original gvdW theory. Nevertheless we include it here, as it has become standard in recent density functional formulations, which implicitly correct for it when excluded volume effects are subsequently considered.

In most practical applications of DFT, one is usually interested in heterogeneous systems, e.g. in the vicinity of particles or surfaces. In this case, the free energy expression can be generalized to include a spatially varying particle density, as follows:

$$\begin{aligned}\beta\mathscr{F}^{\mathrm{MF}}[n(\mathbf{r})] = &\int n(\mathbf{r})(\ln[n(\mathbf{r})] - 1)\,\mathrm{d}\mathbf{r} \\ &+ \frac{\beta}{2}\iint n(\mathbf{r})n(\mathbf{r}')\phi(|\mathbf{r}-\mathbf{r}'|)\,\mathrm{d}\mathbf{r}\,\mathrm{d}\mathbf{r}' \\ &+ \beta\int n(\mathbf{r})V_{\mathrm{ex}}(\mathbf{r})\,\mathrm{d}\mathbf{r}\end{aligned} \tag{2.5}$$

where $V_{\mathrm{ex}}(\mathbf{r})$ is the external potential, which causes the inhomogeneity in the system. This external potential is generated by, e.g. fixed particles or surfaces. Equation (2.5) describes the free energy, as a *functional* of the particle density, which is the source of the expression *density functional theory* (DFT).[1] The equilibrium density profiles are determined by minimizing the free energy functional. In practice, this is often carried out by numerical iteration, as will be explicitly illustrated below. For electrostatic systems, the theory does reasonably well and corresponds precisely to the PBA (to be discussed below). However, it is not accurate in many applications, especially for dense fluids. In that case, we have still to resolve the repulsive core issues in the mean-field energy described earlier. The problem is that, so far, we have not taken account of particle correlations. Consider first the impact of such correlations

[1] It is important to emphasize the *classical* nature of these DFTs, given that quantum mechanical DFTs also are prevalent in the scientific literature. In the latter case, the *energy* (rather than free energy) is a functional of the *electron* (rather than particle) densities. The common use of the acronym "DFT" may lead to some confusion.

on the energy per particle. As we have stated, the mean-field expression leads to a divergence in the energy when the pair potential describes hard cores, as it "allows" configurations where particles overlap one another. Of course, these configurations are forbidden in reality, and such core–core correlations need to be included in the energy term. This was recognized by van der Waals [18], whose original expression for real gas pressures treated the manifestations of the repulsive and attractive parts of the potential separately. Indeed, the *exact* expression for the energy per particle (assuming pairwise additive interactions) in the bulk fluid would be:

$$e_p = 2\pi n_b \int_0^\infty r^2 g(r)\phi(r)\,\mathrm{d}r \tag{2.6}$$

where $g(r)$ is the radial distribution function, which accounts for all particle (including core–core) correlations. The generalization of this expression to non-uniform fluids is obvious in principle, however, an accurate estimate for non-uniform $g(r)$ is normally difficult. Furthermore, its inclusion in the energy term, without a corresponding contribution to the entropy, may lead to an "unbalanced" free energy functional. Noting that removing the repulsive core–core contribution is paramount, we can settle with a very simple approximation, wherein $g(r)$ is modelled as a step function,[2] with the step entering at an interparticle separation d (the hard core diameter). Thus:

$$e_p = 2\pi n_b \int_0^\infty r^2 \phi(r)\theta(r-d)\,\mathrm{d}r \tag{2.7}$$

with

$$\theta(r) = \begin{cases} 1, & r > 0 \\ 0, & r \leq 0 \end{cases} \tag{2.8}$$

where d is the distance of the closest approach between particles; a "hard core diameter". In order to balance this term with an entropy contribution, we should also consider that the introduction of an excluded volume around each particle also reduces the available volume, which we denote as V_{free}. A simple estimate of V_{free}, also inspired by the work of van der Waals, is $V_{\text{free}} = V - Nd^3$, where d^3 is an approximation of the excluded volume per particle. Applying these ideas to the bulk free energy gives:

$$\frac{\beta\mathscr{F}}{V} = n_b \ln\left[\frac{N}{V - Nd^3}\right] - n_b + 2\pi\beta n_b^2 \int_0^\infty r^2\phi(r)\theta(r)\,\mathrm{d}r \tag{2.9}$$

[2] Other alternatives will be considered below, for ionic solutions

This expression for the bulk free energy is surprisingly accurate for simple dense liquids. As above, it is generalized to non-uniform systems, to give:

$$\begin{aligned}\beta\mathscr{F}[n(\mathbf{r})] = &\int_V n(\mathbf{r})(\ln\left[\frac{n(\mathbf{r})}{1-n(\mathbf{r})d^3}\right] - 1)\,\mathrm{d}\mathbf{r} \\ &+ \frac{\beta}{2}\int n(\mathbf{r})\int n(\mathbf{r}')\phi(\mathbf{r},\mathbf{r}')\theta(|\mathbf{r}-\mathbf{r}'|-d)\,\mathrm{d}\mathbf{r}' \\ &+ \beta\int n(\mathbf{r})V_{\mathrm{ext}}(\mathbf{r})\,\mathrm{d}\mathbf{r}. \end{aligned} \tag{2.10}$$

This functional can treat the adsorption of a simple liquid at a wall as well as the gas–liquid interface [17, 19]. Over the years, more accurate treatments, and extensions to polymeric molecules, have been presented.

2.2.1.1 The Fine-Grained GvdW Theory

A major breakthrough in the development of modern DFT was the introduction by Nordholm of a non-local treatment of excluded volume interactions [16]. This innovation allowed the treatment of packing effects (density oscillations), and also resulted in a DFT that fulfils important thermodynamic sum rules, such as the contact value theorem. The key conceptual step was to realize that the excluded volume effect is related to an average particle density over a spatial domain determined by the range of the repulsive interactions. Consider the excluded volume interaction between identical particles, with a hard-sphere diameter d. The simplest coarse-graining average, reflecting the domain of the repulsive interactions, is

$$\overline{n}(\mathbf{r}) = \frac{3}{4\pi d^3}\int_{|\mathbf{r}-\mathbf{r}'|<d} \mathrm{d}\mathbf{r}'\, n(\mathbf{r}')\ . \tag{2.11}$$

Thus, we assume that the excluded volume effect is related to $\overline{n}(\mathbf{r})$. The free energy functional is then given by:

$$\begin{aligned}\beta\mathscr{F}[n(\mathbf{r})] = &\int n(\mathbf{r})(\ln\left[\frac{n(\mathbf{r})}{1-\overline{n}(\mathbf{r})d^3}\right] - 1)\,\mathrm{d}\mathbf{r} \\ &+ \frac{\beta}{2}\int n(\mathbf{r})\int n(\mathbf{r}')\phi(\mathbf{r},\mathbf{r}')\theta(|\mathbf{r}-\mathbf{r}'|-d)\,\mathrm{d}\mathbf{r}' \\ &+ \beta\int n(\mathbf{r})V_{\mathrm{ext}}(\mathbf{r})\,\mathrm{d}\mathbf{r}. \end{aligned} \tag{2.12}$$

This functional is able to describe hard-sphere structuring at hard walls and related phenomena [13, 14, 16]. Nordholm denoted this non-local density functional as the "fine-grained" gvdW. Subsequently, a plethora of other non-local DFT formulations

have appeared in the literature, such as the WDA (Weighted Density Approximation) or SDA (Smoothed Density Approximation). Essentially, all these (including the more recent Fundamental Measure theory, FMT) are based on the same overall principles of non-locality, pioneered by Nordholm [20].

A general expression for the non-local density functional is given by:

$$\begin{aligned}\beta\mathscr{F}[n(\mathbf{r})] = &\int n(\mathbf{r})(\ln[n(\mathbf{r})] - 1)\,\mathrm{d}\mathbf{r} + \int n(\mathbf{r})(\beta f_{\mathrm{HS}}[\{\overline{n}_i(\mathbf{r})\}])\,\mathrm{d}\mathbf{r} \\ &+ \frac{\beta}{2}\int n(\mathbf{r})\int n(\mathbf{r}')\phi(\mathbf{r},\mathbf{r}')\theta(|\mathbf{r}-\mathbf{r}'|-d)\,\mathrm{d}\mathbf{r}' \\ &+ \beta\int n(\mathbf{r})V_{\mathrm{ext}}(\mathbf{r})v\,\mathrm{d}\mathbf{r} \end{aligned} \tag{2.13}$$

where the excluded volume contribution to the free energy (per particle) is estimated by f_{HS}. Note that this term is expressed as a possible functional of several coarse-grained (weighted) densities $\{\overline{n}_i\}$. One example is that suggested by Tarazona and Evans [21]. They based their free energy functional upon the Carnahan–Starling [22] equation of state for hard spheres, i.e.:

$$\beta f_{\mathrm{HS}} = \frac{\eta(4-3\eta)}{(1-\eta)^3}, \tag{2.14}$$

where η is the volume fraction, which is given by $\eta = \pi d^3 n_b/6$ for the bulk fluid. The non-local, or "weighted" particle density was generated as [23, 24]:

$$\overline{n}(\mathbf{r}) = \int \mathrm{d}\mathbf{r}'\, w\big(|\mathbf{r}-\mathbf{r}'|; n(\mathbf{r})\big)n(\mathbf{r}')\ , \tag{2.15}$$

$$w(r) = w_0(r) + w_1(r)n + w_2(r)n^2\ , \tag{2.16}$$

where the weight functions w_i were determined by fitting to the direct correlation function and the radial distribution function, for a uniform hard sphere fluid, as given by the Percus–Yevick integral equation theory.

2.2.2 Grand Potential and Symmetry

The free energy minimization used in DFT leads to an integral equation in general. Thus, problems which can be simplified due to higher symmetries are particularly amenable to treatment. Examples include a single infinite and flat surface, or the interstitial regime between two such surfaces, in which case the average density only depends on the dimension normal to the surface(s), x say. In other words, a mean-field integration of the y, z directions leaves us with $n = n(x)$, which simplifies our problem considerably. Similarly, in systems with spherical symmetry, we end up with $n = n(r)$, and with cylindrical symmetry, $n = n(\rho, x)$.

A common scenario is that the non-uniform system is in equilibrium with a bulk solution, at a fixed chemical potential, μ. A single infinite flat surface immersed in a fluid is a good illustrative example of this. In this case, it is necessary to define a grand potential, $\Omega[n(x)]$, given by:

$$\Omega[n(x)] = \mathscr{F}[n(x)] - \mu \int n(x)\,\mathrm{d}x \tag{2.17}$$

The equilibrium density profile $n_{\mathrm{eq}}(x)$ is the one for which this grand potential is minimized. This equilibrium density is often determined in a simple iterative manner (from the equation $\delta\Omega/\delta n(x) = 0$), though more advanced convergence schemes have also been suggested.

2.3 DFT of Simple Ionic Systems

We shall now focus our discussion on ionic solutions.

2.3.1 Poisson–Boltzmann DFT

The Poisson–Boltzmann Approximation (PBA) follows from the mean-field functional described earlier. Only the Coulomb potential is incorporated in the energy term, thus core–core repulsions are neglected and the energy remains finite. With these assumptions, we arrive at the following free energy functional:

$$\begin{aligned}\beta\mathscr{F}^{\mathrm{PB}}[\{n_\alpha(\mathbf{r})\}] = &\int \sum_\alpha n_\alpha(\ln[n_\alpha(\mathbf{r})] - 1)\,\mathrm{d}\mathbf{r} \\ &+ \frac{\beta}{2}\iint \sum_\alpha \sum_\lambda n_\alpha(\mathbf{r}) n_\lambda(\mathbf{r}')\phi^{\alpha\lambda}_{\mathrm{Coul}}(|\mathbf{r}-\mathbf{r}'|)\,\mathrm{d}\mathbf{r}\,\mathrm{d}\mathbf{r}' \\ &+ \beta\int \sum_\alpha V_{ex}(\mathbf{r}) n_\alpha(\mathbf{r})\,\mathrm{d}\mathbf{r},\end{aligned} \tag{2.18}$$

where n_α is the density of ion species α, while $\phi^{\alpha\lambda}_{\mathrm{Coul}}(r)$ is the Coulomb interaction energy between ions α and λ, separated by a distance r:

$$\beta\phi^{\alpha\lambda}_{\mathrm{Coul}}(r) = l_B \frac{z_\alpha z_\lambda}{r} \tag{2.19}$$

The valency of ion α is denoted by z_α, while $l_B = \beta e^2/(4\pi\varepsilon_0\varepsilon_r)$ is the Bjerrum length. The elementary charge is denoted by e, while ε_0 and ε_r are the permittivity of vacuum and the dielectric constant of the (implicit continuum) solvent, respectively.

2.3.1.1 An Example: Flat Charged Surfaces

Consider two charged and opposing planar surfaces which confine an electrolyte solution [25]. We assume this electrolyte is in equilibrium with a bulk solution. The walls have a uniform surface charge density σ_s and are separated by a distance h. The slit geometry allows analytic integration of $\mathscr{F}[n_\alpha(\mathbf{r})]$ in the (y, z) direction parallel with the surfaces, to obtain $\mathscr{F}[n_\alpha(x)]$. Thus, with μ_α denoting the chemical potential of ion α, we arrive at the following grand potential (at the PB level):

$$\beta\Omega^{\mathrm{PB}} = \beta\mathscr{F}^{\mathrm{PB}} + 2\pi l_B \sigma_s^2 h/e^2 - \sum_\alpha \beta\mu'_\alpha \int_0^h n_\alpha(x')\,\mathrm{d}x' \tag{2.20}$$

where μ'_α is the electrochemical potential. Minimizing the grand potential leads to the following integral equation for the ionic densities in the slit:

$$n_\alpha(x) = e^{\left[2\pi\sigma l_B h z_\alpha + \beta\left(\mu_\alpha + z_\alpha\Psi_D - \sum_\lambda \int_0^h n_\lambda(x')\phi^{\alpha\lambda}_{\mathrm{Coul}}(|x-x'|)\,\mathrm{d}x'\right)\right]} \tag{2.21}$$

which can be solved via Picard iterations where a portion of the previous iteration is mixed with the current one, in order to ensure stable convergence [14]. Here μ_α is the chemical potential of the bulk species. Electroneutrality is maintained by a Donnan potential, Ψ_D (which contributes to the electrochemical potential). Note that the interaction potentials, $\phi^{\alpha\lambda}_{\mathrm{Coul}}(|x|)$, only have to be calculated once, storing the results in a vector.

2.3.2 Approximating Ion Correlations

As discussed above, one of the major advantages of DFT is that it is relatively straightforward to extend the model so as to include other model features, such as excluded volume and dispersion interactions. Additionally, it is also possible to approximate *ion correlations* in cases where they are expected to be important. For example, in systems containing multivalent ions [26–28], including polyelectrolyte solutions. We will briefly describe two methods that we have employed to treat correlations:

- Add a separate term, approximating the correlation free energy, to the functional.
- Use an effective potential, rather than ϕ_{Coul}, designed so as to approximate effects from a spatially varying radial distribution function, between ions of like charge.

The first option has been successfully used in models of room temperature ionic liquids, whereas the latter has been employed for models of aqueous solutions containing salt as well as polyelectrolytes.

2.3.2.1 Adding a Separate Correlation Term

In this case, we assume that the free energy functional has the general form:

$$\beta\mathscr{F}^{\mathrm{CT}}[n_\alpha(\mathbf{r})] = \beta\mathscr{F}^{\mathrm{PB}}[\{n_\alpha(\mathbf{r})\}] + \beta\int\sum_\alpha n_\alpha(\mathbf{r})\, f_c[\bar{n}_\alpha(\mathbf{r})]\,\mathrm{d}\mathbf{r} \tag{2.22}$$

where the index "CT" indicates that we have added a "correlation term" to the PB functional. The quantity, f_c, describes the electrostatic correlation free energy per particle. This can be estimated using concepts derived from the "hole corrected Debye–Hückel" theory [29–34] for the one-component plasma:

$$\begin{aligned} 4\beta f_c[\bar{n}_\alpha(\mathbf{r})] = 1 + \frac{2\pi}{3\sqrt{3}} - \ln[3] + \ln[\omega^2+\omega+1] \\ - \omega^2 - \frac{2}{\sqrt{3}}\tan^{-1}[\frac{2\omega+1}{\sqrt{3}}] \end{aligned} \tag{2.23}$$

where $\omega = [1 + c\bar{n}_\alpha^{1/2}]^{1/3}$ and $c = |\frac{q_\alpha}{e}|^3(3l_B)^{3/2}\sqrt{\frac{4\pi}{3}}$. The "hole corrected Debye–Hückel" theory is summarized in the Appendix.

2.3.2.2 Approximating $g_{\alpha\alpha}(r)$

An alternative approach to adding a separate correlation term, is to introduce correlations directly into the expression for the energy. Here, we describe correlations between like charges, which lead to an "effective Coulomb interaction". The mean-field expression for the electrostatic interaction, Eq. (2.2), includes a "self-interaction" term. At high electrostatic couplings, this self-term is localized and contributes a significant repulsive contribution to the mean-field expression, which should be removed. This can be viewed as a "Coulomb hole" in the like-charge density about a given particle. This is a *soft* hole as particles carrying charges of the same sign naturally tend to avoid each other via the long-ranged Coulomb repulsive force. We shall borrow ideas from earlier work by Forsman and Nordholm [6], and assume a radial distribution function between like charges, $g_{\alpha\alpha}(r)$, with the following properties: $g_{\alpha\alpha}(0) = 0$ and $g_{\alpha\alpha}(r) \to 1$ as $r \to \infty$.

The *like–like* Coulombic interaction (between either anions or cations) is then given by

$$\mathscr{F}^{\mathrm{like}}_{\mathrm{Coul}} = \frac{1}{2}\iint\sum_\alpha n_\alpha(\mathbf{r})n_\alpha(\mathbf{r}')\phi^{\alpha\alpha}_{\mathrm{Coul}}(|\mathbf{r}-\mathbf{r}'|)g_{\alpha\alpha}(|\mathbf{r}-\mathbf{r}'|)\,\mathrm{d}\mathbf{r}'\,\mathrm{d}\mathbf{r} \tag{2.24}$$

Note that these terms may formally diverge in the thermodynamic limit, but a proper accounting of all charges in the system will lead to finite intensive system properties. It should be mentioned, that in some previous works [1, 5], the notation was simplified

by the introduction of an effective interaction potential $\phi_{\text{eff}}^{\alpha\alpha}(r) = \phi_{\text{Coul}}^{\alpha\alpha}(r) g_{\alpha\alpha}(r)$. As a simple approximation for $g_{\alpha\alpha}(r)$, we here choose an exponential form [6–8]:

$$g_{\alpha\alpha}(r) = (1 - e^{-\lambda_\alpha r}) \tag{2.25}$$

The parameter λ_α is determined by a bulk condition of a single particle exclusion:

$$n_\alpha^{(b)} \int \mathrm{d}\mathbf{r}\{g_{\alpha\alpha}(|\mathbf{r}|) - 1\} = -1 \tag{2.26}$$

where $n_\alpha^{(b)}$ is the bulk density of the species α. Thus we obtain,

$$\lambda_\alpha = (8\pi n_\alpha^{(b)})^{1/3} \tag{2.27}$$

A more accurate correction might possibly be obtained, if we allow λ_α to be position dependent (not yet investigated).

2.3.2.3 Accounting for Excluded Volume

It is certainly possible to approximate excluded volume effects, within the DFT framework, by utilizing the concept of fine-grained densities, as described above. There are several different *specific* formulations to estimate excluded volume effects [5, 20, 35–37], but they are fundamentally similar. An important aspect to keep in mind is that upon introducing hard spheres, one is also *effectively* accounting for ion correlations, due to the "interaction hole" (Coulomb hole) that is created by the hard core exclusion. However, a fundamental problem is that this amounts to the approximation of one mechanism (ion correlations) by a totally different mechanism (exchange repulsion). In some systems, particularly at very high salt concentrations, this can lead to accurate predictions, but this accuracy will deteriorate at the more relevant limit of intermediate to low concentrations, since the Coulomb hole then becomes much larger than typical hard core diameters. This has been thoroughly discussed in Ref. [5]. Here, we merely note that in some DFT formulations, estimates of ion correlations *require* the presence of hard cores. Such formulations reduce to a DFT formulation of Poisson–Boltzmann theory (pure mean-field), in the limit of point-like ions. Hence, they will (for instance) completely fail to account for correlation attractions observed in "Swedish double layer" model systems, with charged flat surfaces, and point-like multivalent counterions. These attractions nevertheless exist, as manifested by numerous simulations of these model systems.

Hard sphere excluded volume effects can indeed influence double-layer interactions at short range, but essentially only for monovalent salt, and relatively large ions [1, 38]. In the presence of multivalent ions, these effects are typically small, since the Coulomb repulsion prevents close encounters between multivalent species, carrying charges of the same sign. An illustration is provided in Fig. 2.1, where predictions

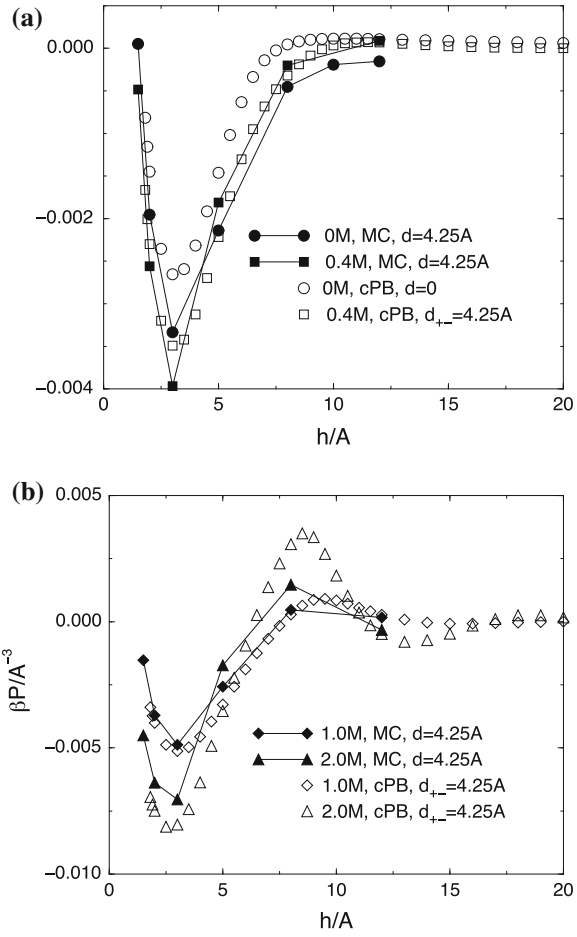


Fig. 2.1 Predictions of the net osmotic pressure in a double-layer system, with two flat and charged surfaces, immersed in a 2:1 salt solution, where the divalent species is counterion to the charged surfaces. The surface charge density is given by $e/\sigma = -60\,\text{Å}^2$ and the simulated ions carried a hard-core diameter $d = 4.25\,\text{Å}$. MC simulation data from Åkesson et al. [38]. The acronym "cPB" denotes "correlation-corrected Poisson–Boltzmann theory, which utilizes a soft "Coulomb hole" between ions of like charge, in a manner similar to that described in the main text. Reprinted with permission from Ref. [1]. Copyright (2004) American Chemical Society

by a correlation-corrected DFT, not incorporating hard-sphere exclusion effects, are compared with corresponding simulations of interactions between charged surfaces in an electrolyte containing hard-sphere ions.[3] Specifically, the solution contained a 2:1 salt, and the surfaces were negative. We see that substantial excluded volume effects were only found at 2M 2:1 salt, which amounts to an exceptionally high ionic strength. In fact, under such conditions, electrostatic interactions are almost completely screened out anyway.

Since this review focuses on interactions at the mean-field level, with possible improvements to account for ion correlations, we will not provide detailed descriptions of excluded volume effects, and how to incorporate them in our DFT formulations. This has been thoroughly described in earlier works [5, 35, 37].

[3] The correlation correction was estimated in a somewhat different manner from our suggestion above, but based on similar ideas.

2.4 Examples

We provide calculations on two different model systems, illustrating some relevant features of the DFT approach.

2.4.1 Interaction Between Two Charged Colloidal Particles

This is a very simple model system, but appropriate for illustrative purposes. We study the potential of mean force between two charged spherical particles, immersed in salt solutions. Dispersion interactions are neglected, but can of course be added, for instance under standard Hamaker assumptions. In order to highlight the accuracy of the mean-field PB approximation itself, for these systems, we will also include corresponding results obtained via Metropolis Monte Carlo (MC) simulations. In the latter case, the simulation box was cylindrical, with hard but inert cylinder surfaces, and without any periodic boundary conditions. Simulations were performed at fixed discrete particle separations, whereby the average force was sampled. Force statistics were improved by imposing a soft, rather that hard, repulsion from the particle surfaces, acting on the surrounding ions: $\beta V_{\rm ex}(r) = (\delta/(r - R_C))^6$, where r is the distance to the particle origin, whereas $R_C = 40\,\text{Å}$, and $\delta = 6\,\text{Å}$. Ions were not allowed to penetrate regions for which $r \leq R_{\rm ref}$. The Bjerrum length was $l_B = 7.16\,\text{Å}$. Each particle had a valency of $Z_C = -100$. In the DFT calculations, bulk conditions are "automatically" approached far away from the particles, due to the grand canonical formulation. Hence, such calculations do not require any artificial enclosing surface. Nevertheless, the symmetry of the system implies a cylindrical symmetry of the average density, i.e. $n = n(z, \rho)$, with z defined as an axis through the centres of the particles. The system is pictorially illustrated in Fig. 2.2.

We have analyzed the net electrostatic double-layer force, at bulk salt concentrations of 10 and 40 mM. The results are presented in Fig. 2.3, where we compare PB predictions (from DFT calculations) with corresponding data from MC simulations. As is well known, the mean-field PB treatment leads to an overestimation of the double-layer repulsion. However, a significant improvement results if we invoke some reasonable simple estimate of correlations between ions of like charge, using ideas similar to those discussed above. This has been thoroughly explored in earlier work [1, 5], and will be demonstrated for polyelectrolyte solutions below.

We have already emphasized how useful it is that DFT treatments, including the PB version, fulfil important thermodynamic sum rules. For instance, the net force acting between the particles, matches the one obtained by discrete differentiation of the free energy. An example is shown in Fig. 2.4. We emphasize that this is not only satisfactory from a fundamental point of view, but also serves as a useful check of the DFT code.

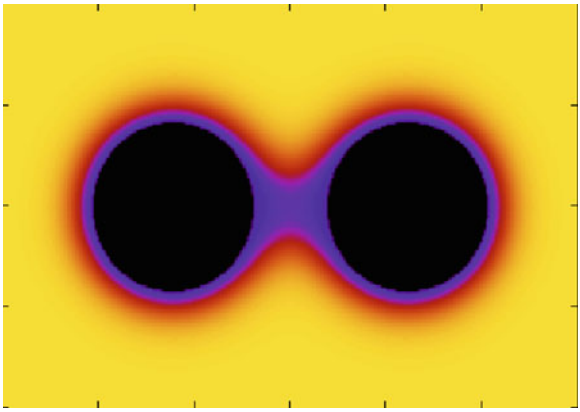


Fig. 2.2 Ion densities, surrounding the two charged particles. The ion concentration is given by a colour, with *yellow* representing the bulk value, while *black* indicates a vanishing density. The z-axis runs through the particle centres, while ρ is perpendicular to z

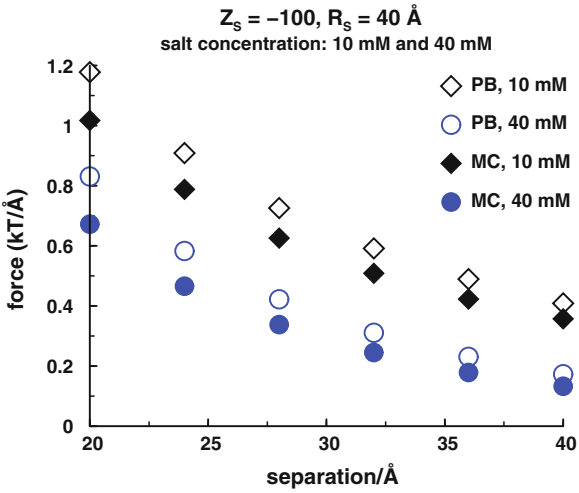


Fig. 2.3 Net electrostatic force between the two charged particles (see text), as predicted by PB (DFT calculations), and established by MC simulations, respectively. The separation is measured with respect to the surfaces of the particles, defined to be located at $R_c = 40$ Å from the respective origin

2.4.2 Adsorption of Polyions to Oppositely Charged Surfaces

Here, we shall briefly recapitulate some results obtained in an earlier work [7], where DFT predictions of polyion adsorption were compared with MC simulation data. In order to facilitate simulations of relatively realistic chain lengths, electrostatic

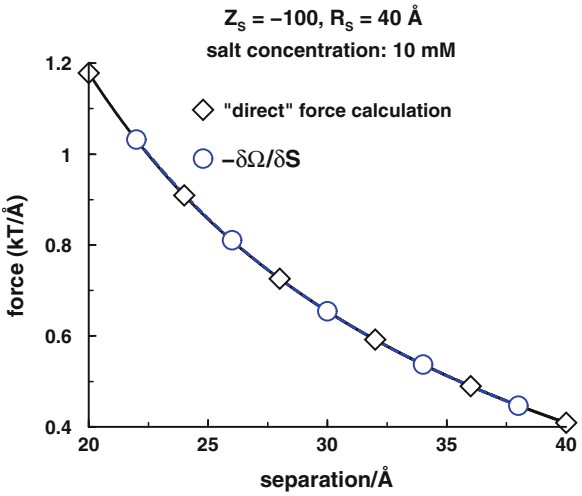


Fig. 2.4 Demonstrating that the "contact value theorem" (generalized to soft potentials) is fulfilled

interactions were handled at the linearised PB level, i.e. via a screened Coulomb potential [39]. In other words, with all monomers carrying a unit charge, the electrostatic interaction, $u_{\rm mm}(r)$, is given by:

$$\beta u_{\rm mm} = \frac{l_B e^{-\kappa r}}{r} \tag{2.28}$$

where r is the monomer–monomer separation, whereas $\kappa^2 = 2\frac{\beta c_S e^2}{\varepsilon_r \varepsilon_0}$, with c_S denoting the bulk concentration of monovalent salt ($l_B = 7.16\,$Å). This means that κ^{-1} is the Debye screening length. The net adsorption of monomers at a single charged sphere, of radius $R_c = 100\,$nm, carrying a total charge of $Q_c = -8657e$. These values were inspired by an experimental work [40]. The electrostatic monomer–particle interaction, $u_{\rm mc}$, can be written as [41]:

$$\beta u_{\rm mc} = l_B z_c \frac{\sinh(\kappa R_c)}{\kappa R_c} \frac{e^{-\kappa r}}{r} \qquad (r > R_c) \tag{2.29}$$

Similarly to our previous example, monomers are repelled near the surface of the particle by a soft potential, $w(r)$ with $\beta w(r) = (\delta/(r - R_c))^6$, although in this case, $\delta = 5\,$Å. The total particle–monomer interaction is thus, $V_{\rm ex}(r) = u_{\rm mc}(r) + w(r)$. As we shall demonstrate, ion correlations are extremely important in these systems. Hence, an approximation of the monomer–monomer radial distribution function was included in the DFT treatment, as described by Eqs. (2.25–2.27). Connectivity was treated using a version of the polymer DFT, originally introduced by Woodward [12].

The net adsorption of monomers, Γ_{net}, was defined as:

$$\Gamma_{\text{net}} = \frac{\int_{R_c+d}^{\infty} r^2 (n(r) - n_b)\, \mathrm{d}r}{R_c^2} \tag{2.30}$$

where r is the distance from the origin, at which the charged particle resides. A parameter d effectively removes undesired contributions from the trivial exclusion regime, close to the particle surface, brought about by the soft repulsion, $w(r)$. It was set to $d = 4\,\text{Å}$, but the results are insensitive to this choice.

The work focused on the way in which the net adsorption depends on the bulk concentration of simple salt, n_b. The main results are collected in Fig. 2.5. We see that the simulated dependence is qualitative, and even semi-quantitatively, reproduced

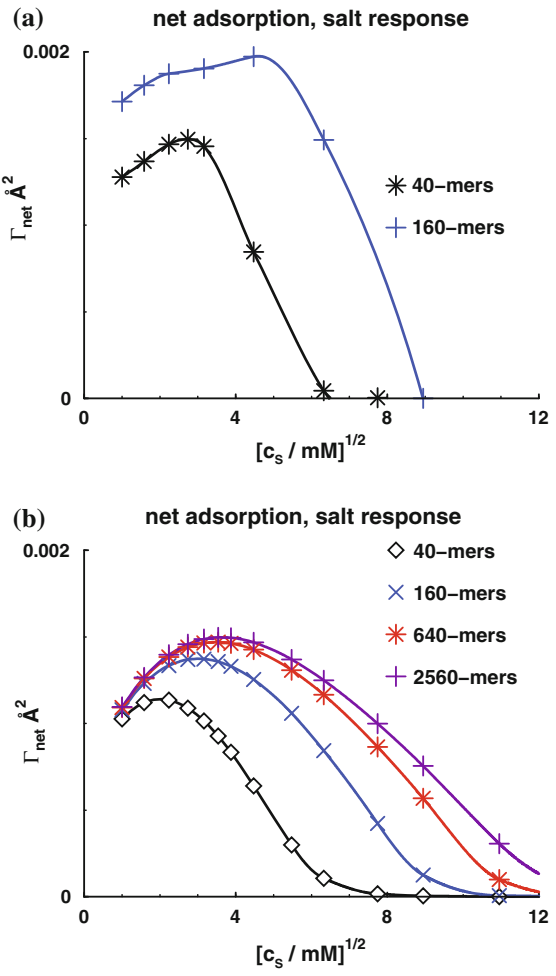


Fig. 2.5 Responses of the net adsorption, to changes of the salt concentration. **a** Γ_{net}, for 40-mers and 160-mers, across the full simulated range of salt concentrations. **b** DFT predictions of Γ_{net}, for various degrees of polymerization. Reprinted, with permission from Langmuir **28**, 5138 (2012). Copyright 2012, American Chemical Society

by the correlation-corrected DFT. If these were to be compared with experimental data, say from ellipsometry measurements, the discrepancy between DFT and MC data would be negligible, compared to other aspects, such as poorly known surface charge density, the "translation" of measured angles to net adsorption, polydispersity, non-electrostatic contributions to adsorption, etc. The computational power of the DFT approach allows us to approach the long chain limit, where the results no longer change (essentially), as the molecular weight of the polymers increase. We can summarize the observations found from Fig. 2.5 as follows. At low ionic strengths the adsorption increases with salt concentration, since the reduced charged repulsion allows more (positive) charges to pack at the (negative) surface. Above some threshold salt level, however, the reduced electrostatic attraction to the surface instead dominates, and the net adsorption starts to drop. This threshold concentration is higher when the polymers are long, and at intermediate ionic strengths, short chains can display a dramatically weaker adsorption than long ones.

2.4.2.1 Importance of Ion Correlations

We can easily reduce our correlation-corrected DFT to the corresponding pure mean-field version, simply by setting $g_{\mathrm{mm}} = 1$ everywhere. The role played by correlations can thus be evaluated, via comparisons between predictions by the mean-field, and the correlation-corrected DFT versions. This is exemplified in Fig. 2.6, displaying the net adsorption of long chains (2,560-mers) at various salt concentrations. Notice how the mean-field version predicts an overall too weak adsorption. More importantly, the very *existence* of an adsorption maximum is lost at the mean-field level! This

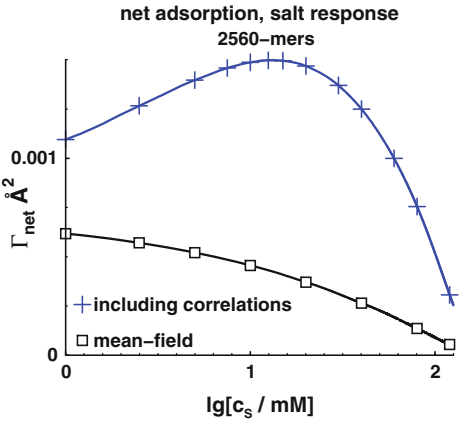


Fig. 2.6 DFT predictions of how the net adsorption responds to salt addition, for 2,560-mers. *Crosses* are data from calculations with the full, correlation-corrected DFT, while *squares* show results obtained when the correlation part is removed (the mean-field version). Notice that we here have used a logarithmic scale for the salt. Reprinted with permission from Langmuir **28**, 5138 (2012). Copyright 2012, American Chemical Society

illustrates why previous mean-field studies have concluded that such a maximum only can exist if there is some additional *non-electrostatic* attraction to the surface. In other words, some approximate treatment of ion correlations is for these systems *required*, for a theory to produce qualitatively correct predictions. Mean-field approaches fail due to the way in which they *overestimate the repulsion between like-charged species* (in our case monomers) [1]. This overestimate disfavours adsorption, and the resulting error grows with the degree of correlations in the system. On the other hand, at very weak screening, the "Coulomb hole" effectively prevents charges from packing densely at the surface, which is what we observe in the "screening-enhanced" regime, at low salt levels.

2.5 Conclusions

Numerical methods to solve the PB equation are well developed, for a range of different scenarios and boundary conditions. While classical DFT approaches are more juvenile, they do sometimes offer important advantages, particularly regarding the versatile way in which it can accommodate connected molecules, ion correlations and non-electrostatic interactions. We hope that present and future work in this area will promote classical DFT as a significant complementary tool to standard (differential equation) PB, for studies of ionic solutions.

Appendix: The Hole Corrected Debye–Hückel Theory

We include a summary of the Debye–Hückel hole (DHH) theory, closely following the original descriptions [29–34]. This entails a correlation-corrected theory of the one-component plasma, OCP. In the OCP, one charged species is treated explicitly, whereas the other serves as a neutralizing background charge. Let us assume that the explicit ions carry a charge q (valency z), and that the bulk density is n_b. We will furthermore put a "tagged" particle at the origin. The (configurational) free energy can then be expressed as a functional of the ion density surrounding our central ion:

$$\beta\mathscr{F}[n(\mathbf{r})] = \int n(\mathbf{r})(\ln n(\mathbf{r}) + 1)\,\mathrm{d}\mathbf{r} \; + \; z^2 l_B \int \Delta n(\mathbf{r}) \left(\frac{1}{2} \int \frac{\Delta n(\mathbf{r}')}{|\mathbf{r} - \mathbf{r}'|} d\mathbf{r}' + \frac{1}{|\mathbf{r}|}\,\mathrm{d}\mathbf{r} \right) \tag{2.31}$$

where $\Delta n(\mathbf{r}) = n(\mathbf{r}) - n_b$ is the deviation of the ion density from its bulk value. Minimizing this functional leads to the anticipated Boltzmann distribution:

$$n(r) = n_b e^{-\beta q \psi(r)} \tag{2.32}$$

where the potential ψ is given by:

$$\psi(r) = \frac{q}{4\pi\varepsilon_0\varepsilon_r}\left(\frac{1}{r} + \int \frac{\Delta n(\mathbf{r}')}{|\mathbf{r}-\mathbf{r}'|}\,\mathrm{d}\mathbf{r}'\right) \tag{2.33}$$

Upon linearisation, we end up at the Debye–Hückel level:

$$\Delta n(r) = \frac{-\kappa^2\exp(-\kappa r)}{4\pi r}, \qquad \beta\kappa^2 = \frac{n_b q^2}{\varepsilon_0\varepsilon_r}. \tag{2.34}$$

The electrostatic coupling strength, Γ, is a convenient dimensionless quantity, defined as:

$$\Gamma = \frac{l_B z^2}{a} \tag{2.35}$$

where $a = \left(4\pi n_b/3\right)^{-1/3}$ measures the radius of a spherical volume per particle. The (potential) energy per particle, u, can be neatly expressed in terms of Γ:

$$\beta u = -\frac{\sqrt{3}}{2}\,\Gamma^{3/2} \tag{2.36}$$

A charge integration gives us the electrostatic free energy per particle, f:

$$\beta f = \beta\int_0^\Gamma \frac{\mathrm{d}\Gamma'}{\Gamma'}\,u(\Gamma') = -\frac{1}{\sqrt{3}}\Gamma^{3/2} \tag{2.37}$$

At this Debye–Hückel level, the radial distribution function is:

$$g_{\mathrm{DH}}(r) = 1 - \frac{\kappa^2}{4\pi n_b}\frac{1}{r}\exp(-\kappa r)\ . \tag{2.38}$$

As Nordholm pointed out [31], $g_{\mathrm{DH}}(r)$ becomes negative at small r, which of course is unphysical. In the DHH theory, this is avoided via the introduction of a correlation hole, of radius h, surrounding the central ion:

$$g(r) = \begin{cases} 0, & r < h \\ 1 - \dfrac{h}{r}\exp\big(-\kappa(r-h)\big), & r \geq h \end{cases}\ . \tag{2.39}$$

The size of the "hole" is adjusted, such that it contains one ion, assuming a uniform bulk density n_b:

$$n_b \int_0^\infty \mathrm{d}r\, 4\pi r^2 \big(1 - g(r)\big) = 4\pi n_b \left[\frac{h^3}{3} + \int_h^\infty \mathrm{d}r\, rh \exp\big(-\kappa(r-h)\big) \right] = 1. \quad (2.40)$$

Thus:

$$h = \kappa^{-1} \left[\left(1 + (3\Gamma)^{3/2} \right)^{1/3} - 1 \right]. \quad (2.41)$$

With the introduction of such a hole, the electrostatic energy becomes:

$$\beta u = -\frac{1}{4} \left[\left(1 + (3\Gamma)^{3/2} \right)^{2/3} - 1 \right]. \quad (2.42)$$

whereas a charge integration gives:

$$\beta f = \frac{1}{4} \left(1 + \frac{2\pi}{3\sqrt{3}} + \ln\left(\frac{\omega^2 + \omega + 1}{3} \right) - \omega^2 - \frac{2}{\sqrt{3}} \arctan\left(\frac{2\omega + 1}{\sqrt{3}} \right) \right), \quad (2.43)$$

where

$$\omega = \left(1 + (3\Gamma)^{3/2} \right)^{1/3}. \quad (2.44)$$

The DHH theory has proven remarkably accurate for a range of different coupling strengths [33], and model systems [29, 30, 32, 34].

References

1. Forsman J (2004) A simple correlation-corrected Poisson–Boltzmann theory. J Phys Chem B 108:9236
2. Woodward CE, Forsman J (2004) Density functional study of surface forces in solutions containing star-shaped polymers. Macromolecules 37:7034
3. Woodward CE, Forsman J (2008) Density functional theory for polymer fluids with molecular weight polydispersity. Phys Rev Lett 100:098301
4. Kurut A, Henriques J, Forsman J, Skepö M, Lund M (2013) Role of histidine for charge regulation of unstructured peptides at interfaces and in bulk. Proteins 81:1097
5. Forsman J (2009) Density functional theories of salt solutions. J Chem Phys 130:064901
6. Forsman J, Nordholm S (2012) Polyelectrolyte mediated interactions in colloidal dispersions: hierarchical screening, simulations and a new classical density functional theory. Langmuir 28:4069
7. Forsman J (2012) Polyelectrolyte adsorption: electrostatic mechanisms and nonmonotonic responses to salt addition. Langmuir 28:5138
8. Xie F, Nylander T, Utsel S, Wågberg L, Åkesson T, Forsman J (2013) Polyelectrolyte adsorption on solid surfaces: theoretical predictions and experimental measurements. Langmuir 29:712421
9. Frink LJD, Salinger AG (2000) Two- and three dimensional nonlocal density functional theory for inhomogeneous fluids. I. Algorithms and parallelizations. J Comp Phys 159:407

10. Frink LJD, Salinger AG (2000) Two- and three dimensional nonlocal density functional theory for inhomogeneous fluids. II. Solvated polymers as a benchmark problem. J Comp Phys 159:425
11. Knepley MG, Karpeev DA, Davidivits S, Eisenberg RS, Gillespie D (2010) An efficient algorithm for classical density functional theory in three dimension: ionic solutions. J Chem Phys 132:124101
12. Woodward CE (1991) A density functional theory for polymers: application to hard chain-hard sphere mixtures in slitlike pores. J Chem Phys 94:3183
13. Freasier BC, Woodward CE, Nordholm S (1989) Generalized van der Waals theory of hard sphere oscillatory structure. J Chem Phys 90:5657
14. Freasier BC, Nordholm S (1983) A generalized van der Waals model for solvation forces between solute particles in a colloidal suspension. J Chem Phys 79:4431
15. Nordholm S, Haymet ADJ (1980) Generalized van der Waals theory. I. Basic formulation and application to uniform fluids. Aust J Chem 33:2013
16. Nordholm S, Johnson M, Freasier BC (1980) Generalized van der Waals theory. III. The prediction of hard sphere structure. Aust J Chem 33:2139
17. Nordholm S, Gibson J (1981) Generalized van der Waals theory. VII. Interface profiles and surface tension. Aust J Chem 34:2263
18. van der Waals JD (1873) Over de Continuïteit van den Gas—en Vloeistoftoestand, thesis, Leiden
19. Johnson M, Nordholm S (1981) Generalized van der Waals theory. VI. Application to adsorption. J Chem Phys 75:1953
20. Wu J, Zhidong L (2007) Density functional theory of complex fluids. Ann Rev Phys Chem 58:85
21. Tarazona P, Evans R (1984) A simple density functional theory for inhomogeneous liquids. Mol Phys 52:847
22. Carnahan NF, Starling KE (1969) Equation of state for nonattracting rigid spheres. J Chem Phys 51:635–636
23. Evans R (1992) Density functionals in the theory of nonuniform fluids. In: Henderson D (ed) Fundamentals of inhomogeneous fluids. Marcel Dekker, New York, pp 85–175. ISBN 0-8247-8711-0
24. Tarazona P (1984) A density functional theory of melting. Mol Phys 52:81
25. Gouy G (1910) Sur la constitution de la charge electrique ala surface d'un electrolyte. J Phys 9:457
26. Guldbrand L, Jönsson B, Wennerström H, Linse P (1984) Electrical double layer forces. A Monte Carlo study. J Chem Phys 84:2221
27. Kjellander R, Marcelja S (1984) Correlation and image charge effects in electric double layers. Chem Phys Lett 112:49
28. Kjellander R, Åkesson T, Jönsson B, Marcelja S (1992) A comparison of the anisotropic HNC and Monte Carlo simulations. J Chem Phys 97:1424
29. Abbas Z, Gunnarsson M, Ahlberg E, Nordholm S (2001) Corrected Debye–Hückel analysis of surface complexation. I. Bulk salt limit. J Colloid Interface Sci 243:11–30
30. Abbas Z, Gunnarsson M, Ahlberg E, Nordholm S (2002) Corrected Debye–Hückel theory of salt solutions: size asymmetry and effective diameters. J Phys Chem B 106:1403
31. Nordholm S (1984) Simple analysis of the thermodynamic properties of the one-component plasma. Chem Phys Lett 105:302
32. Penfold R, Nordholm S, Jönsson B, Woodward CE (1990) A simple analysis of ion-ion correlation in polyelectrolyte solutions. J Chem Phys 92:1915
33. Penfold R, Nordholm S, Jönsson B, Woodward CE (1991) A simple analysis of the classical hard sphere one component plasma. I. Hole corrected Debye–Hückel theory. J Chem Phys 95:2048
34. Penfold R, Nordholm S, Nichols N (2005) Simple analysis of the thermodynamic properties for classical plasmas. J Stat Mech: Theory Expt, P06009. ISSN 1742–5468
35. Nordholm S (1984) Generalized van der Waals theory. XII. Application to ionic solutions. Aust J Chem 37:1

36. Rosenfeld Y (1993) Free energy model for inhomogeneous fluid mixtures: Yukawa-charged hard spheres, general interactions, and plasmas. J Chem Phys 98:8126
37. Tang Z, Scriven LE, Davis HT (1992) Interactions between primitive electrical double layers. J Chem Phys 97:9258
38. Åkesson T, Jönsson B (1991) Monte Carlo simulations of colloidal stability—beyond the Poisson-Boltzmann approximation. Electrochim Acta 36:1723
39. Debye P, Hückel E (1923) De la theorie des electrolytes. I. Abaissement du point de congelation et phenomenes associes. Phys Z 24:185–206
40. Hierrezuelo J, Szilagyi I, Vaccaro A, Borkovec M (2010) Probing nanometer-thick polyelectrolyte layers adsorbed on oppositely charged particles by dynamic light scattering. Macromolecules 43:9108
41. Beresford-Smith B, Chan DYC, Mitchell DJ (1985) The electrostatic interaction in colloidal systems with low added electrolyte. J Coll Int Sci 105:216

Springer

http://www.springer.com/978-3-319-12210-6

Computational Electrostatics for Biological Applications
Geometric and Numerical Approaches to the Description of Electrostatic Interaction Between Macromolecules

Rocchia, W.; Spagnuolo, M. (Eds.)

2015, XII, 306 p. 92 illus., 73 illus. in color., Hardcover
ISBN: 978-3-319-12210-6